Ageing and memory in the relaxation dynamics of collections of two-level subsystems

2005 J. Phys.: Condens. Matter 17 3343

(http://iopscience.iop.org/0953-8984/17/21/027)

INSTITUTE OF PHYSICS PUBLISHING JOURNAL OF PHYSICS: CONDENSED MATTER

J. Phys.: Condens. Matter **17** (2005) 3343–3354 doi:10.1088/0953-8984/17/21/027

Ageing and memory in the relaxation dynamics of collections of two-level subsystems

C A Viddal and R M Roshko

Department of Physics and Astronomy, University of Manitoba, Winnipeg, MB, R3T 2N2, Canada

Received 23 February 2005, in final form 22 April 2005
Published 13 May 2005
Online at stacks.iop.org/JPhysCM/17/3343

Abstract

The relaxation dynamics of collections of interacting, thermally activated, two-level subsystems are shown to be characterized by nonequilibrium ageing and memory effects which are analogous to those observed in magnetic systems where randomness and frustration yield a collectively frozen magnetic state with spin-glass-like correlations. Numerical simulations of these nonequilibrium relaxation effects are presented and compared with measurements performed on assemblies of nanodimensional magnetic particles, and their physical origins, as well as their relationship to genuinely collective nonequilibrium relaxation phenomena, are discussed within a theoretical framework based on the Preisach model of hysteresis.

1. Introduction

Assemblies of nanodimensional magnetic particles with a sufficiently high particle density exhibit anomalous relaxation dynamics [1, 2], which mimic those observed in canonical spin glasses like AgMn [3]. Principal among these are ageing, with and without temperature cycling, and memory. Ageing refers to the observation that the magnetic response of a nanoparticulate assembly depends on the time t_a for which the system is held at constant temperature following cooling from the high temperature superparamagnetic phase, and is visible directly as a relaxation of the moment (or the frequency dependent susceptibility) in the cooling field [2], or as an age dependence of the relaxation isotherms following field application or removal [1]. If ageing at temperature T is temporarily interrupted by negative temperature cycling to $T - \Delta T$, the ageing process is effectively suspended for the duration of the cycling, while positive temperature cycling to $T + \Delta T$ erases the ageing and restores the system to a 'younger' configuration [2, 4]. Memory refers to the observation that if field cooling is temporarily halted and the system is aged at constant temperature T for a time t_a before cooling is resumed then the magnetic response exhibits an upward 'step' at the ageing temperature T when the system is subsequently warmed from low temperatures [2]. Anomalous relaxation effects like these are interpreted as evidence that dipole–dipole interactions between the magnetic nanoparticles

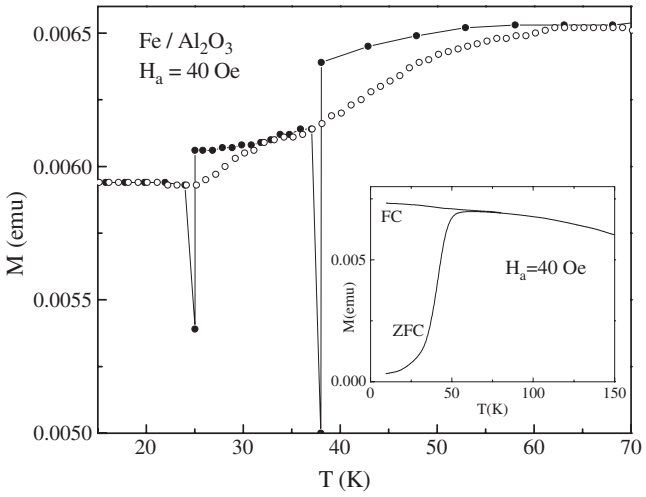

Figure 1. Memory steps in the measured field cooled moment of nanoparticles of Fe in Al_2O_3 as described in the text. Solid circles are cooling data; open circles are warming data. The inset shows the temperature dependence of the measured FC and ZFC moments in $H_a = 40$ Oe.

induce a collective 'super-spin-glass' state, with a multivalley free energy landscape in which the energy barriers describe collective metastable state excitations, rather than single-particle excitations. (The concept of a dipolar spin glass is not new, and efforts to disentangle relaxation effects which are superparamagnetic in origin from those which are uniquely characteristic of collective dipolar freezing can be traced back to the classic studies of Eiselt *et al* [5, 6] and Tholence *et al* [7] on dilute $Eu_xSr_{1-x}S$, where magnetically rigid, internally exchange-coupled clusters of Eu ions exhibit two distinct dynamic anomalies, a 'high temperature' anomaly, which is attributed to the thermal blocking of individual clusters, and a 'low temperature' anomaly, which has been linked to intercluster coupling.)

Recently, another class of memory experiments has appeared in the literature [8], which claims to support not only the existence of a collective state but, more specifically, a hierarchical organization of metastable states [9], which bifurcates continuously with decreasing temperature, in preference to domain-growth pictures based on the two-state droplet model of Fisher and Huse [10]. The latter experiments, which are illustrated in figures 1 and 2 for a thin film of nanodimensional Fe particles embedded in alumina, are distinguished by field removal and reapplication. The closed circles in figure 1 show the moment of the Fe/Al_2O_3 system measured while cooling from 300 to 10 K at 2 K min^{-1} in a field $H_a = 40$ Oe, with temporary pauses at $T = 38$ and 25 K, during which the field is removed, and the system is aged in zero field for $t_a = 15\,000$ s, followed by field reapplication. When the system is subsequently warmed from 10 K in the field $H_a = 40$ Oe at the same rate of 2 K min^{-1}, the measured moment exhibits a series of upward 'memory steps' which are coincident with the ageing temperatures, as shown by the open circles in figure 1. A similar memory effect is observed in the time dependence of the moment, when relaxation at $T = 35$ K, following zero-field cooling and the application of a field $H_a = 40$ Oe, is interrupted after a period of 5000 s by negative temperature cycling to $T = 25$ K with field removal, for a further period of 5000 s, and then back to $T = 35$ K with field reapplication. As figure 2 shows, aside from a brief recovery phase, the time dependence of the moment after reheating is a smooth continuation of the initial time dependence. (This effect is asymmetric, in the sense that

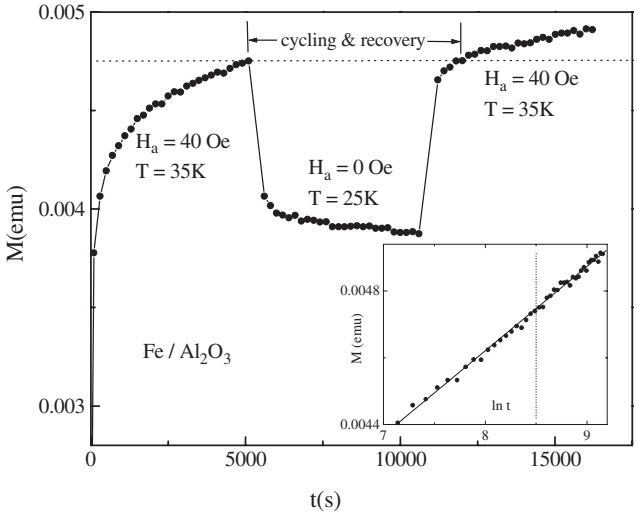

Figure 2. Memory in the measured relaxation of the zero-field cooled moment of Fe/Al_2O_3 at $T = 35$ K in $H_a = 40$ Oe, interrupted by negative temperature cycling to $T = 25$ K with field removal. The inset shows the moment plotted on a logarithmic timescale, with the temperature cycling and recovery phase removed.

positive temperature cycling from T to $T + \Delta T$ and back to T does *not* restore a continuation of the initial relaxation.) In spite of the suggestive structural similarities between the relaxation responses in figures 1 and 2, and those observed in strongly coupled systems with spin-glass-like correlations, the relaxation phenomena presented here are, as we will show, a characteristic of nonequilibrium dynamics in any magnetic system for which the temperature dependence of the magnetic response is dominated by thermal-fluctuation-driven moment reversals over a fixed distribution of free energy barriers, and are thus *not necessarily* collective in origin. While similar conclusions have been reached by other investigators [11, 12], working in the hypothetical limit of no interactions, the physical origin of these effects is not properly understood, nor is their dependence on interparticle interactions or their sensitivity to the details of the experimental protocol. In the current investigation, we study the relaxation response of a model system composed of a collection of thermally activated, interacting, two-level subsystems, subject to the temperature and field cycling protocols described above. We show that such systems exhibit nonequilibrium ageing and memory phenomena, which are highly reminiscent of those observed in systems where randomness and frustration yield a collectively frozen magnetic state with spin glass correlations, but which differ in certain fundamental respects from relaxation dynamics which are genuinely collective in origin.

2. Model simulations

The representation of magnetic materials as collections of elementary bistable subsystems was first introduced into the literature by Preisach [13], and has since evolved into a general mathematical and physical framework for the description of hysteresis and irreversibility in a wide variety of magnetic materials, including ferromagnets, spin glasses, and superparamagnets [14–17]. The subsystems represent the Barkhausen instabilities which are fundamental to all magnetizing processes, and each Barkhausen subsystem is characterized by a moment μ, two magnetic states $\pm\mu$, and by a double-well free energy profile in a two-state

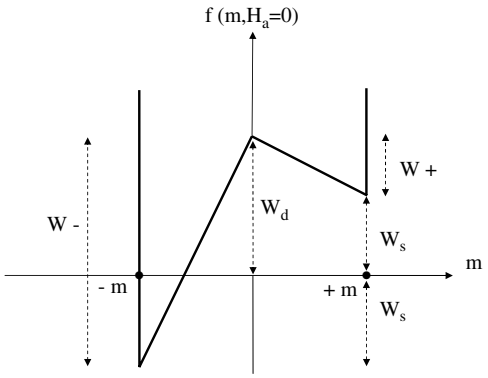

Figure 3. The free energy profile of a two level subsystem with two magnetic configurations $\pm\mu$, and two excitation barriers W_+ and W_-, or equivalently, a dissipation barrier W_d and a level splitting W_s.

configuration space, shown in figure 3, with two excitation barriers for moment reversal W_+ and W_-, or equivalently a dissipation barrier $W_d = (W_+ + W_-)/2$, which describes the energy lost irreversibly as heat in a Barkhausen transition, and a level splitting $2W_s = W_- - W_+$, which describes the energy stored reversibly in a transition. Thermally activated overbarrier transitions are driven by a thermal viscosity field $H_T = H_f \ln(t_{exp}/\tau_0)$, where $H_f = kT/\mu$ is the thermal fluctuation field and t_{exp} is the experimental time constant, and a specific magnetic material is described by a distribution $p(H_d, H_s)$ of subsystem characteristic fields $H_d = W_d/\mu$ and $H_s = W_s/\mu$. The field H_s is typically interpreted as an *interaction* field, although this is by no means a necessary consequence of the formalism.

The state of the entire ensemble of subsystems in a field H_a at a temperature T, following a specific history of field and temperature excursions, has an elegant geometrical representation in the Preisach plane, defined by orthogonal coordinate axes H_d and H_s. A given experimental protocol is represented by a state boundary which partitions the plane into $+\mu$ and $-\mu$ subregions. The Preisach diagrams for standard protocols like field cooling (FC) followed by field removal, and zero-field cooling (ZFC) followed by field application and removal, have been discussed in detail in the literature [17], and are reproduced here with limited justification.

2.1. Memory in the FC moment with field removal

We begin by discussing the Preisach representation of the FC memory effect illustrated in figure 1. At sufficiently high temperatures such that the thermal fluctuation energy $W_T = k_T \ln(t_{exp}/\tau_0)$ exceeds both excitation barriers W_+ and W_- of a given subsystem, the subsystem is in thermal equilibrium and responds superparamagnetically to an applied field, with an induced moment given by

$$m_{eq} = \mu \tanh\left[\frac{\mu(H_a - H_s)}{kT}\right]. \tag{1}$$

When the temperature is lowered, the subsystem will fall out of equilibrium at the blocking temperature T_B where the thermal energy W_T matches the lower excitation barrier [17, 18] $W_d = \mu(H_d - |H_s - H_a|)$, which yields

$$T_B = \frac{\mu(H_d - |H_s - H_a|)}{k \ln(t_c/\tau_0)} \tag{2}$$

where t_c is the appropriate experimental field cooling time constant. For all temperatures $T < T_B$, the subsystem level populations are frozen at $\exp[\pm(H_a - H_s)/kT_B]$ and the subsystem

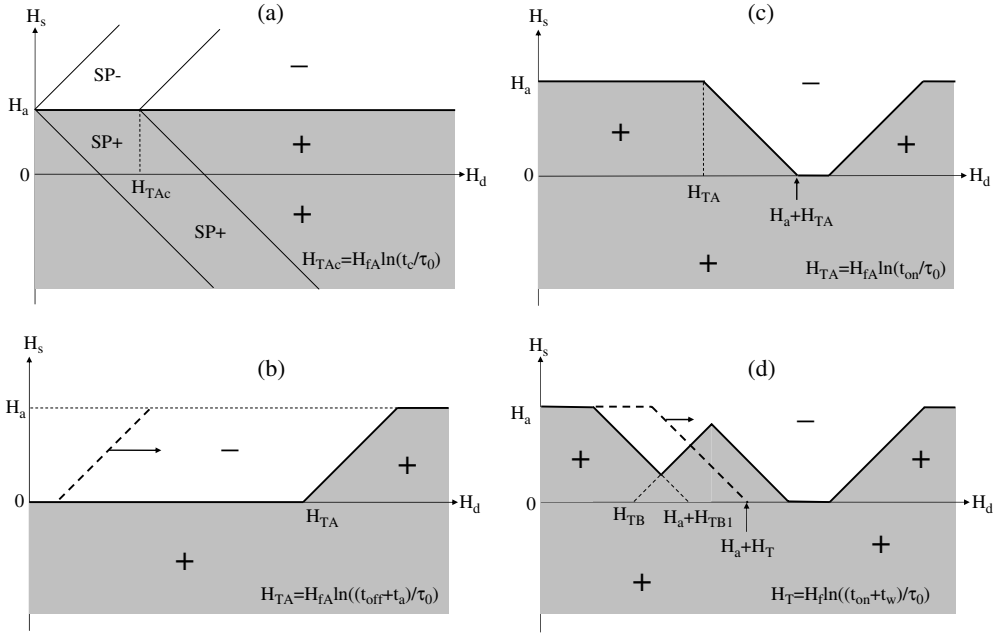

Figure 4. Preisach representation of the experimental protocol which results in memory steps in the field cooled moment. (a) Preisach representation of the field cooled state. (b) Preisach diagram for field removal at temperature T_A followed by ageing for a time t_a. (c) Preisach diagram for field reapplication at temperature T_A followed by cooling to T_B. (d) A repetition of the same field removal, ageing, and field application sequence at temperature T_B, followed by warming from low temperatures (dashed boundary).

moment is frozen at

$$m_{\text{blocked}} = \mu \tanh\left[\frac{\mu(H_a - H_s)}{kT_B}\right] = \mu \tanh\left[\frac{(H_a - H_s)\ln(t_c/\tau_0)}{H_d - |H_s - H_a|}\right]. \tag{3}$$

For typical experimental cooling times $t_c \sim 100$ s, $\ln(t_c/\tau_0) \sim 20$–25, the hyperbolic tangent in equation (3) is negligibly different from unity for all but those subsystems which lie within a narrow strip $|H_a - H_s| \leqslant H_d/15$ in the Preisach plane. For the current purposes, all such departures from unity can be ignored, and it is sufficient to set $m_{\text{blocked}} = \pm\mu$. Figure 4(a) shows the Preisach representation of the field cooled (FC) state. The bold black line separating the shaded (positive moment) and unshaded (negative moment) areas is the state boundary. The subsystems in the regions labelled SP are superparamagnetic, with moments given by equation (1). This superparamagnetic component contributes a temperature dependence which has no direct relevance to the specific memory effect discussed here and, consequently, for computational and conceptual simplicity, we replace m_{eq} by the saturation moment $\pm\mu$. The total system moment is a sum of all the individual subsystem moments $m(H_d, H_s)$, each weighted by the Preisach density $p(H_d, H_s)$:

$$M(H_a, T) = \int_{-\infty}^{+\infty} \mathrm{d}H_s \int_0^{\infty} \mathrm{d}H_d\, m(H_d, H_s)\, p(H_d, H_s). \tag{4}$$

It follows from an inspection of figure 4(a) that the model FC moment is a constant, independent of temperature. Figure 4(b) shows the Preisach diagram for field removal at a temperature T_A, with experimental time constant t_{off}, followed by ageing for a time t_a, where the thermal fluctuation field is $H_{fA} = kT_A/\mu$, and the thermal viscosity field is

$H_{TA} = H_{fA} \ln[(t_{off} + t_a)/\tau_0] \cong H_{fA} \ln(t_a/\tau_0)$, since experimentally, $t_a \gg t_{off}$. The dashed boundary shows the initial location of the state boundary after field removal is complete and before ageing has begun ($t_a = 0$). Figure 4(c) shows the Preisach diagram for field reapplication at the same temperature T_A, followed by cooling. The thermal viscosity field H_{TA}, and hence the shape and location of this particular segment of the state boundary, are determined entirely by a single time constant, the experimental time t_{on} for field turn-on and stabilization, so that $H_{TA} = H_{fA} \ln(t_{on}/\tau_0)$. Figure 4(d) shows the final configuration of the state boundary (bold line) following field cooling from T_A to T_B, where the thermal fluctuation field is $H_{fB} = kT_B/\mu < H_{fA}$, and a repetition of the same field removal/reapplication sequence, where $H_{TB} = H_{fB} \ln[(t_{off} + t_a)/\tau_0]$ and $H_{TB1} = H_{fB} \ln(t_{on}/\tau_0)$. Thus field cooling interrupted by ageing in zero field is distinguished from simple field cooling (figure 4(a)) by a Preisach state boundary with 'notches', whose relative locations and depths are determined by the ratio of the ageing temperatures T_A/T_B, by the applied field H_a, and also by the details of the experimental protocol through the experimental time constants t_{on} and t_{off}. Figure 4(d) also shows the Preisach representation of the final step in the experimental protocol, in which the system is warmed from low temperatures, with a warming time constant $t_w \ll t_a$, comparable to the cooling time constant t_c. The dashed boundary, which intersects the H_d-axis at $H_a + H_T = H_a + (kT/\mu) \ln[(t_{on} + t_w)/\tau_0]$, sweeps through the Preisach plane with increasing temperature T, inverting the moments of the subsystems in the 'notches' from $-\mu$ to $+\mu$ and thus restoring the FC state just prior to field removal and ageing. The restoration begins at the ageing temperature, and proceeds gradually until the system reaches a temperature at which the entire 'notch' is inverted. In particular, a comparison of figures 4(c) and (d) shows that the inversion of the lower temperature T_B-notch, and the restoration of the FC state at T_B, will be complete when $H_f \ln[(t_{on} + t_w)/\tau_0] \approx H_{fA} \ln(t_{on}/\tau_0)$, that is, when $T \approx T_A$. It is also clear from an inspection of these Preisach constructions that this particular memory effect is sensitive to the details of the experimental protocol and, furthermore, that some memory steps (like the T_B-step) demand the existence of subsystems with nonvanishing bias fields H_s, and thus are observable only in magnetic systems with interacting components, while other memory steps (like the T_A-step), for which the Preisach state boundary includes a segment of the H_d-axis, are observable in noninteracting systems as well. However, in neither case is the existence of a collectively ordered state a prerequisite for observing memory steps in the FC moment. Figure 5 shows a numerical simulation of the memory effect based on the Preisach diagrams in figure 4, assuming a lognormal–Lorentzian Preisach density

$$p(H_d, H_s) = (2\pi\sigma_d^2 H_d^2)^{-1/2} \exp[-(\ln(H_d/\bar{H}_d))^2/2\sigma_d^2] \cdot (\sigma_s/\pi)[H_s^2 + \sigma_s^2]^{-1} \tag{5}$$

with $\bar{H}_d = 300$ Oe (typical of real nanoparticulate assemblies), $\sigma_d = 0.5$, and $\sigma_s = 60$ Oe, and with parameters $H_a = 40$ Oe, $T_A = 35$ K, $T_B = 20$ K, $k/\mu = 0.3$ Oe/K (corresponding to a subsystem moment $\mu \sim 5 \times 10^4 \mu_B$), $t_a = 15\,000$ s, and $t_w = t_c = 100$ s. The inset in the figure shows a numerical simulation of the temperature dependence of the model FC and ZFC moments in a field $H_a = 40$ Oe, which includes the superparamagnetic temperature dependence neglected in the memory simulation, and provides a context for the memory step sequence in the main body of the figure. The simulation clearly reproduces the essential features of the measurement in figure 1.

2.2. Memory in relaxation isotherms with temperature cycling

By following a similar procedure, it is possible to construct the Preisach representation of the experimental protocol which leads to the relaxation memory effect illustrated in figure 2.

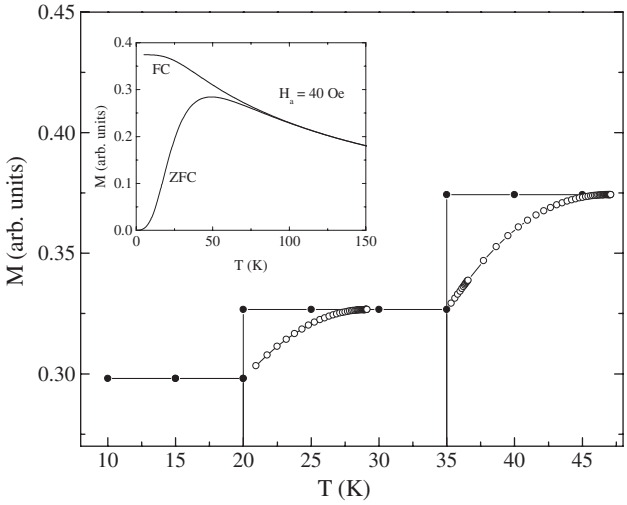

Figure 5. Model simulations of memory steps in the field cooled moment in a field $H_a = 40$ Oe, following ageing in zero field at $T_A = 35$ K and $T_B = 20$ K during cooling, as described in the text. The inset shows the temperature dependence of the model FC and ZFC moments in a field $H_a = 40$ Oe.

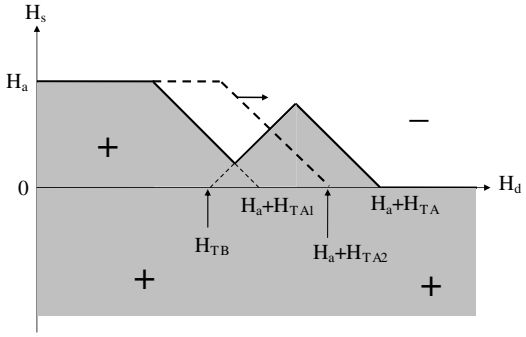

Figure 6. Preisach representation of the experimental protocol for relaxation interrupted by temperature cycling, as described in the text. The bold line shows the location of the Preisach boundary at the instant the field has been reapplied following temperature cycling from T_A to T_B and back to T_A. The dashed boundary describes the subsequent relaxation of the moment as a function of observation time t.

The entire experimental sequence is summarized in figure 6. The thermal viscosity field $H_{TA} = H_{fA} \ln[(t_{on} + t_a)/\tau_0]$ shows the location of the Preisach state boundary after zero field cooling to T_A where $H_{fA} = kT_A/\mu$, followed by the application of a field with time constant t_{on}, and ageing for t_a. The field $H_{TB} = H_{fB} \ln[(t_{off} + t_a)/\tau_0]$ shows the location of the Preisach boundary after field cooling from T_A to T_B, where $H_{fB} = kT_B/\mu$, followed by field removal with time constant t_{off}, and ageing for t_a. Since $H_{fB} < H_{fA}$, little relaxation is expected to occur at T_B, apart from the initial decrease related to the field removal. When the system is warmed back to T_A and the field H_a is reapplied, the system does *not* immediately return to the state which it occupied at the end of the first ageing process, since the relevant viscosity field at the instant that field reapplication is complete is $H_{TA1} = H_{fA} \ln(t_{on}/\tau_0) < H_{fA} \ln[(t_{on} + t_a)/\tau_0]$. Thus the system moment, at the instant when relaxation recommences, defined by the bold

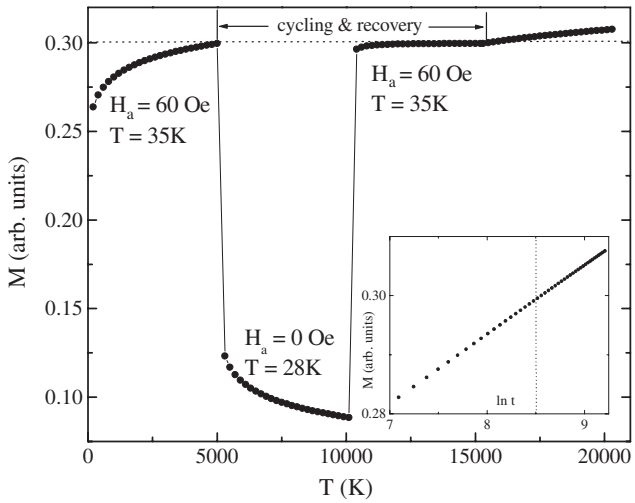

Figure 7. Model simulations of the relaxation of the zero-field cooled moment at $T_A = 35$ K in a field $H_a = 60$ Oe, interrupted by temperature cycling to $T_B = 28$ K in zero field.

Preisach boundary in figure 6, lies somewhat below the value reached at the termination of the first ageing process, and only recovers this value after a further time t_a has elapsed, and the dashed boundary defined by $H_a + H_{TA2} = H_a + H_{fA} \ln[(t_{on} + t_a)/\tau_0]$ is coincident with the initial ageing boundary at $H_a + H_{TA}$. Beyond this point, the relaxation becomes a *smooth continuation* of the relaxation in the first ageing interval, and all memory of the intermediate ageing process is wiped out. Thus memory in the current sense, after temperature cycling and field removal, is once again seen to be a simple consequence of thermally activated dynamics over a distribution of independent energy barriers, rather than a cooperative phenomenon. Figure 7 shows a numerical Preisach simulation of this memory effect assuming the lognormal–Lorentzian Preisach distribution in equation (5) with distribution parameters $\bar{H}_d = 300$ Oe, $\sigma_d = 0.5$, and $\sigma_s = 60$ Oe, and with $H_a = 60$ Oe, $k/\mu = 0.3$ Oe/K, $T_A = 35$ K, $T_B = 28$ K, $t_c = t_w = 100$ s, and $t_a = 5000$ s. The inset shows that the relaxation after the initial conditions have been restored, and following a recovery phase, is a smooth continuation of the initial relaxation isotherm. According to the model, the recovery phase is an essential consequence of the warming and field reapplication protocol, cannot be superposed on the initial relaxation by a simple time shift, and must be completed before the true continuation of the initial relaxation can be observed. It is also clearly a characteristic of the measured memory data in figure 2.

2.3. Ageing in the field cooled moment of blocked superparamagnets

One of the signatures of canonical spin glasses like CuMn is the dependence of the magnetic state on the age of the system, that is, on the time t_a for which the system is held at *constant temperature* T in a *constant field* H_a following cooling from above the glass temperature [19]. In particular, the field cooled (FC) moment is observed to relax monotonically upward at 'high' temperatures, monotonically downward at 'low' temperatures [19], and nonmonotonically downward and then upward at intermediate temperatures. Similar ageing phenomena have also been observed in higher density systems of nanoparticles [2], and have been interpreted as evidence of cooperative freezing of the dipole–dipole coupled nanoparticle moments into an orientationally random, frustrated spin-glass-like configuration.

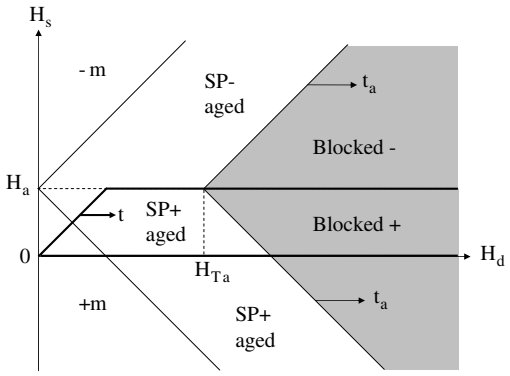

Figure 8. Preisach representation of the ageing of the field cooled state of a collection of two-level subsystems. The bold boundaries show the Preisach representation of field removal and relaxation of the thermoremanent moment from the aged FC state.

However, ageing is also a characteristic of simple superparamagnetic blocking, where the relaxation dynamics are governed by individual thermally activated moment reversals over a spectrum of independent energy barriers. As before, the physical reasons for this are particularly easy to appreciate within the Preisach framework. For a given two-level subsystem, blocking occurs during cooling, at a temperature T_B such that $H_{TB} = (kT_B/\mu)\ln(t_c/\tau_0) = (H_d - |H_s - H_a|)$, where t_c is a time constant defined by the experimental cooling rate. If the subsystem is subsequently cooled to a lower temperature $T < T_B$ and then aged at this lower temperature for a time t_a, the thermal viscosity field H_T will grow with ageing time t_a as $H_T = (kT/\mu)\ln[(t_c + t_a)/\tau_0]$, and the subsystem will *unblock* when $H_T = H_{TB}$, that is, at a time t_a such that

$$(kT/\mu)\ln[(t_c + t_a)/\tau_0] = (kT_B/\mu)\ln(t_c/\tau_0). \tag{6}$$

At this time, the subsystem moment will jump discontinuously from its blocked value in equation (3) to its unblocked superparamagnetic value m_{SP} in equation (1), where $|m_{SP}| > |m_{blocked}|$, so that

$$\Delta m = \mu \tanh\left[\frac{\mu(H_a - H_s)}{kT}\right] - \mu \tanh\left[\frac{\mu(H_a - H_s)}{kT_B}\right]. \tag{7}$$

For subsystems with $H_s < H_a$, $m_{blocked}$ and m_{SP} are positive, as is Δm, while, for subsystems with $H_s > H_a$, $m_{blocked}$, m_{SP}, and Δm are all negative. The total moment of the entire ensemble will thus vary continuously with the age t_a of the ensemble, with the precise behaviour depending upon the relative weighting of the two types of subsystems. Figure 8, if we ignore the bold boundaries, shows the Preisach representation of this ageing process. Subsystems in the regions labelled 'SP + aged' and 'SP − aged' are unblocked and have reached thermal equilibrium during the ageing time t_a, while subsystems in the shaded regions are blocked in their field cooled configurations. Numerical simulations of the age dependence of the moment have been performed for a system with a lognormal distribution of dissipation fields, and for various bias field distributions $g(H_s)$:

$$p(H_d, H_s) = (2\pi\sigma_d^2 H_d^2)^{-1/2}\exp[-(\ln(H_d/\bar{H}_d))^2/2\sigma_d^2]\cdot g(H_s) \tag{8}$$

with $\bar{H}_d = 300$ Oe, and $\sigma_d = 0.5$, and with $H_a = 1$ Oe, $T = 60$ K and $k/\mu = 0.3$ Oe/K, and these simulations are summarized in figure 9(a). If $g(H_s)$ is a single symmetric Gaussian distribution:

$$g(H_s) = (2\pi\sigma_s^2)^{-1/2}\exp[-H_s^2/2\sigma_s^2] \tag{9}$$

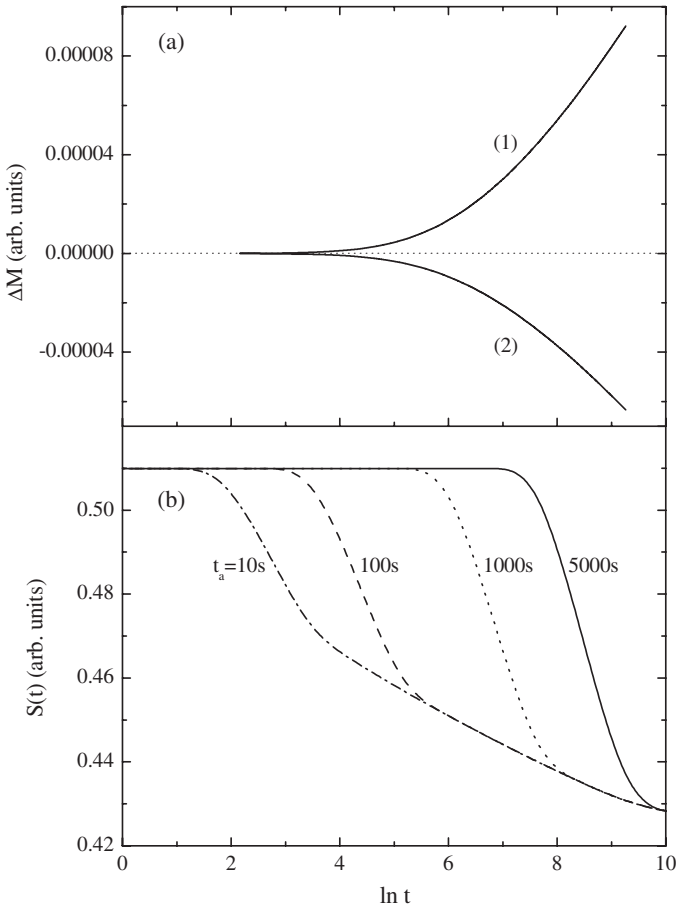

Figure 9. (a) Numerical Preisach simulations of the ageing of the field cooled moment with time t at constant temperature T in a constant field H_a for (1) a single symmetric Gaussian distribution of bias fields H_s and (2) a bimodal Gaussian distribution of bias fields H_s. (b) Numerical Preisach simulations of the relaxation rate $S \equiv -\partial M/\partial \ln t$ as a function of $\ln t$ for TRM relaxation isotherms obtained by ageing at a constant temperature (corresponding to a thermal fluctuation field $H_f = 20$ Oe) in a constant field $H_a = 1$ Oe for ageing times $t_a = 10$, 100, 1000, and 5000 s, followed by field removal.

with $\sigma_s = 60$ Oe, the difference between the aged moment and the field cooled moment:

$$\Delta M = \int \mathrm{d}H_d \int \mathrm{d}H_s \, \Delta m p(H_d, H_s) \tag{10}$$

with Δm given by equation (7), relaxes *upward* with time t_a, while if $g(H_s)$ is a *bimodal* Gaussian, with two peaks symmetrically located about $H_s = 0$:

$$g(H_s) = \tfrac{1}{2}(2\pi\sigma_s^2)^{-1/2}\{\exp[-(H_s - \bar{H}_s)^2/2\sigma_s^2] + \exp[-(H_s + \bar{H}_s)^2/2\sigma_s^2]\} \tag{11}$$

and with $\bar{H}_s = 60$ Oe and $\sigma_s = 60$ Oe, then the system moment relaxes *downward* from its field cooled value. A crossover from upward to downward relaxation has been observed in spin glasses with cooling [19], while, to our knowledge, only downward relaxation has been observed in nanoparticulate assemblies [2]. However, recent micromagnetic simulations [20] of strongly coupled, high density systems of uniaxial, single-domain nanoparticles have shown

that, under certain circumstances, the distribution of interparticle interaction fields exhibits a *bimodal structure* when the system is in a low moment configuration, due to the formation of internally coupled clusters of nanoparticles which switch rigidly as a unit. When viewed in combination with the ageing simulations presented above, this suggests that the ageing of the FC state observed in *some* nanoparticulate assemblies may well be a noncollective, superparamagnetic effect, in which interactions between the individual components *must be present*, and must be distributed in a particular way, but are otherwise *local* in character.

Furthermore, memory of this ageing process is preserved in TRM relaxation isotherms when the field is subsequently removed from the aged FC state. Figure 8 also shows the configuration of the Preisach plane at the instant of field removal. The subsystems which will contribute to the relaxation of the moment with time are those which lie in the region $0 \leqslant H_s \leqslant H_a$ and bounded by the bold lines. These subsystems are trapped in metastable positive moment configurations and will suffer moment reversal as the thermal viscosity boundary $H_T = (kT/\mu)\ln(t/\tau_0)$ propagates to the right with observation time t, as shown. The aged subsystems in the area labelled 'SP + aged' are in the highest-moment configuration compatible with thermal equilibrium at temperature T, $m_{SP+aged} = \mu \tanh[\mu(H_a - H_s)/kT]$, and will experience the most significant moment reversal to the zero-field configuration $m_{SPzero} = -\mu \tanh(\mu H_s/kT)$, in comparison with the blocked subsystems in the shaded region labelled 'Blocked +', which are trapped in lower moment configurations $m_{blocked} = \mu \tanh[\mu(H_a - H_s)/kT_B] < m_{SP+aged}$, and which will contribute progressively smaller moment reversals with increasing H_d, and hence with increasing observation time t. Thus, the TRM relaxation isotherm will exhibit a drop in the decay rate in the vicinity of $t \approx t_a$, when plotted on a logarithmic timescale, and this crossover will become progressively sharper as $H_a \to 0$, and the spread in crossover times, defined by the diagonal boundary separating the 'SP + aged' and 'Blocked +' regions, becomes narrower. Numerical simulations of TRM relaxation isotherms were performed assuming $k/\mu = 0.3$ Oe/K, $T = 60$ K (corresponding to $H_f = 20$ Oe), $H_a = 1$ Oe, $t_c = 1$ s, and a constant Preisach density $p(H_d, H_s)$. The simulations include the effects of thermal broadening. That is, the usual assumption that an individual subsystem relaxes as a step-function on a logarithmic timescale is replaced by a more realistic representation in which moment reversal is spread over a time interval $\Delta \ln t \sim 1$, which is equivalent to limiting the resolution of the subsystem excitation fields H_{exc} to an interval on the order of the thermal fluctuation field $\Delta H_{exc} \sim H_f$. As expected, the model relaxation isotherms are characterized by a smooth 'bend' at an observation time $\ln t \sim \ln t_a$, separating two regimes where the moment decays approximately logarithmically with time. This translates into an age-dependent 'knee' in the relaxation rate $S \equiv -\partial M/\partial \ln t$, as shown in figure 9(b), with systematics which are highly reminiscent of those observed in some nanoparticulate assemblies within the blocked phase, particularly at higher temperatures [1, 21]. The curvature of the knee is determined primarily by thermal broadening, which tends to dominate any smoothing effects related to the dispersion of crossover times mentioned earlier, particularly for fields $H_a \leqslant H_f$. Thus the structure in the relaxation rate in figure 9(b) becomes more diffuse as the temperature increases, and this too is a characteristic of the experimental data.

3. Summary

The relaxation dynamics of collections of interacting, thermally activated, two-level subsystems are shown to be characterized by nonequilibrium ageing and memory effects which are analogous to those observed in magnetic systems where randomness and frustration yield a collectively frozen magnetic state with spin-glass-like correlations. In particular, collections of two-level subsystems exhibit 'memory steps' in the temperature dependence of the field

cooled moment, and memory in the time dependence of TRM relaxation isotherms, as well as an age dependence of the magnetic response at a fixed temperature in a fixed field. However, in spite of superficial similarities, there is one subtle, yet fundamental distinction, which is particularly easy to appreciate when viewed from the perspective of the Preisach formalism, between ageing and memory effects characteristic of superpositions of bistable elements and those which are genuinely collective in origin. If cooling in a field (zero or nonzero) from the high temperature equilibrium (superparamagnetic) phase to a temperature T in the irreversible phase is followed by ageing at temperature T in a *fixed field*, and then by cooling to a lower temperature *without* changing the field, then according to figure 8, memory of the ageing at T is *erased* in bistable ensembles during cooling, as the diagonal boundaries propagate back to the left and reblock the aged superparamagnetic subsystems. Thus a *change in field* is an essential ingredient of the experimental protocol if memory of ageing at constant temperature is to be imprinted permanently on a blocked superparamagnet. (These considerations do not apply to the first two memory effects discussed in sections 2.1 and 2.2, where ageing is always associated with a field change, and is imprinted through moment *reversal*.) By contrast, in systems with collective spin glass correlations, this imprint is achieved by the simple expedient of *waiting*, and reflects the essentially chaotic nature of the frozen state. Of course, these differences do not disqualify any of the relaxation processes described here as potential *contributors* to the nonequilibrium phenomena observed in spin glasses, and in some nanoparticulate assemblies which are believed to exhibit collective behaviour, but they do allow us to classify these phenomena into those which are necessarily collective versus those which are not.

References

[1] Jonsson T, Mattson J, Djurberg C, Khan F A, Nordblad P and Svedlindh P 1995 *Phys. Rev. Lett.* **75** 4138
[2] Jönsson P, Hansen M F and Nordblad P 2000 *Phys. Rev.* B **61** 1261
[3] Jonsson T, Jonason K, Jönsson P and Nordblad P 1999 *Phys. Rev.* B **59** 8770
[4] Djurberg C, Jonason K and Nordblad P 1999 *Eur. Phys. J.* B **10** 15
[5] Eiselt G, Kotzler J, Maletta H, Stauffer D and Binder K 1979 *Phys. Rev.* B **19** 2664
[6] Tholence J L, Holtzberg F, Godfrin H, Lohneysen H V and Tournier R 1978 *J. Physique Coll.* **39** C6 928
[7] Binder K and Young A P 1986 *Rev. Mod. Phys.* **58** 801
[8] Sun Y, Salamon M B, Garnier K and Averback R S 2003 *Phys. Rev. Lett.* **91** 167206
[9] Lefloch F, Hammann J, Ocio M and Vincent E 1992 *Europhys. Lett.* **18** 647
[10] Fisher D S and Huse D A 1988 *Phys. Rev.* B **38** 373
Fisher D S and Huse D A 1998 *Phys. Rev.* B **38** 386
[11] Sasaki M, Jönsson P E, Takayama H and Nordblad P 2004 *Phys. Rev. Lett.* **93** 139701
[12] Zheng R K, Gu H and Zhang X X 2004 *Phys. Rev. Lett.* **93** 139702
[13] Preisach F 1935 *Z. Phys.* **94** 277
[14] Néel L 1950 *J. Physique et Le Radium* **11** 49
[15] Souletie J 1983 *J. Physique* **44** 1095
[16] Bertotti G 1998 *Hysteresis in Magnetism* (New York: Academic)
[17] Song T, Roshko R M and Dahlberg E D 2001 *J. Phys.: Condens. Matter* **13** 3443
[18] Stancu A and Spinu L 1998 *IEEE Trans. Magn.* **34** 3867
[19] Jonsson T, Jonason K and Nordblad P 1999 *Phys. Rev.* B **59** 9402
[20] Stancu A, Stoleriu L, Postolache P and Cerchez M 2004 *IEEE Trans. Magn.* **40** 2113
[21] Jonsson T, Nordblad P and Svedlindh P 1998 *Phys. Rev.* B **57** 497